Supporting Information

Cencic et al. 10.1073/pnas.1011477108

SI Materials and Methods

Ultra-high-throughput screening in 1,536-well format. A time resolved (TR)- fluorescence resonance energy transfer (FRET) based high-throughput assay that monitors the interaction between eIF4E and eIF4G has been previously described (1). The assay is in a homogenous format and has been further miniaturized and optimized for ultra-high-throughput screening (uHTS) in 1,536-well format. To this end, His_6-tagged eIF4E (4.8 nM) and glutathione S-transferase (GST)-tagged $eIF4GI_{517–606}$ (100 nM) were incubated with 1 nM Eu-W1024 labeled anti-6xHis antibody and 50 nM anti-GST IgG antibody conjugated to SureLight-Allophycocyanin (APC) (Perkin Elmer) in TR-FRET buffer (20 mM $Tris_{7.5}$, 50 mM NaCl, and 0.01% NP40). Reactions were dispensed into black 1,536-well plates (Corning Costar 3724#) using a Multidrop Combi (Thermo-Fisher Scientific). Compounds were added using a Beckman NX liquid handling station (Beckman Coulter). Reactions were incubated at room temperature (RT) for 3 h and TR-FRET signal was measured using an Envision multilabel plate reader (Perkin Elmer Life Sciences) with laser excitation at 337 nm and emission filters at 615/8.5 nm and 665/7.5 nm, as well as a LANCE/DELFIA dual mirror (D400/D630). A delay time of 50 μs was used. Due to the time delay, only the longer-lived FRET signal is detected, eliminating short-lived background fluorescence.

FRET signals were expressed as FRET ratios: FRET = F665 nm (fluorescence counts at 665 nm emission)/F615 nm (fluorescence counts at 615 nm emission) * 10,000 cps. Each plate contained DMSO positive control reactions, as well as negative control reactions with His-eIF4E, His-Eu, and GST-APC but no GST-$eIF4GI_{517–606}$. Data were analyzed using BioAssay software (CambridgeSoft). Percent inhibition was calculated for each plate using the equation: $\%\text{Inhibition} = 100 - (\text{FRET}_{\text{compound}} - \text{FRET}_{\text{negative control}} / \text{FRET}_{\text{positive control}} - \text{FRET}_{\text{negative control}})$. $\text{FRET}_{\text{compound}}$ was the FRET ratio from wells with a test compound, $\text{FRET}_{\text{positive control}}$ was an average FRET ratio from wells containing DMSO, defining the maximum FRET within each plate, and $\text{FRET}_{\text{negative control}}$ was the average FRET ratio from wells containing reactions without GST-$eIF4GI_{517–606}$, defining the minimum FRET within each plate. Compounds that caused >30% inhibition were defined as active.

Using this miniaturized TR-FRET assay, a library of 217,341 compounds was screened with the Molecule Library Screening Center Network. The plate Z' values were all above 0.6 and S/B ratios above 10. The primary hit rate was 0.37%. From the primary screen, 798 compounds were identified as inhibiting the TR-FRET signal by at least 30% (Fig. 1*A*). The primary data are available at: http://pubchem.ncbi.nlm.nih.gov/assay/assay.cgi?aid=782&loc=ea_ras.

Synthesis of cpd 4E1RCat and analogs. 4E1RCat, 4-[(3E)-3-[[5-(4-nitrophenyl)furan-2-yl]methylidene]-2-oxo-5-phenylpyrrol-1-yl] benzoic acid, is commercially available through various vendors. This probe compound was identified in the primary uHTS and the activity of the probe compound was confirmed by resynthesis as outlined in Fig. S7.

Synthetic 4E1RCat: ^{1}H NMR (400 MHz, DMSO-d_6) δ: 12.96 (s, 1 H), 8.27 (d, J = 9.4 Hz, 2 H), 8.02 (d, J = 8.6 Hz, 2 H), 7.88 (d, J = 8.6 Hz, 2 H), 7.52 (d, J = 3.9 Hz, 1 H), 7.36-7.30 (m, 4 H), 7.27 (m, 2 H), 7.17 (m, 3 H), 6.80 (s, 1 H); ^{13}C NMR (100 MHz, DMSO-d_6) δ: 169.1, 167.4, 154.9, 154.1, 147.6, 147.1, 140.1, 135.3, 130.8, 130.5, 130.3, 129.5, 129.4, 128.5, 128.2, 127.7, 126.8, 125.6, 125.3, 117.6, 114.5, 104.3; LC/MS-ESI (m/z): $[M + H]^+$ calculated for C28H19N2O6, 479.1; found, 479.0.

To explore the SAR (structure-activity relationship) for 4E1RCat, several analogs were synthesized or purchased. The strategies for chemical modifications of 4E1RCat focused on modifications of parts A and B in the structure (Fig. S1*A*). All synthetic analogs of 4E1RCat were prepared by two step synthesis utilizing cyclodehydration (2) and microwave assisted aminolysis reaction (Fig. S7). Especially, the final aminolysis reaction was carried out using microwave conditions, which were modified and optimized to be more convenient and more efficient. As a result, the reaction was improved in terms of reaction time and yield compared to the previously reported typical aminolysis reaction (3). For modification of part A, various substituents, such as nitro, methoxy, and halogens (Cl, Br), with different substitution positions were introduced. In part B, different positional substitutions of carboxylic acid and other substituents around the phenyl ring were investigated to determine the significance of carboxylic acid for activity of the compound. Based on these modification strategies, a total of 10 synthetic and 6 commercial analogs were prepared.

Modeling of 4E1RCat and eIF4E. The site that binds 4E1RCat was identified using computational solvent mapping of the three-dimensional structures of eIF4E (4). The method places molecular probes—small organic molecules containing various functional groups—on a dense grid defined around the protein, finds favorable positions using empirical free energy functions, refines the selected poses by free energy minimization, clusters the low energy conformations, and ranks the clusters on the basis of the average free energy (4, 5). We used 16 small molecules as probes (ethanol, isopropanol, tert-butanol, acetone, acetaldehyde, dimethyl ether, cyclohexane, ethane, acetonitrile, urea, methylamine, phenol, benzaldehyde, benzene, acetamide, and N,N dimethylformamide). To determine the binding site, we first find consensus sites, i.e., regions on the protein where clusters of different probes overlap, and rank these sites in terms of the number of overlapping probe clusters. The highly ranked consensus sites define energetically important binding regions or hot spots (6). The main hot spot with the largest number of probe clusters and other hot spots within a 7 Å radius predict the site that can potentially bind drug-size ligands (4).

The available X-ray structures of human eIF4E were downloaded from the Protein Data Bank and were mapped after removing all other molecules. The only a priori constraint was blocking the m^7GTP binding site, but 4E1RCat does not compete with the mRNA cap. Based on the mapping, a box for docking was created around this putative binding site with 4 Å padding on each side. The initial atomic coordinates of 4E1RCat were based on the conformer provided by PubChem, but the molecule was considered flexible in docking. The ligand and receptor were prepared for docking using version 1.5.4 of MGLtools, the graphical front-end for setting up and running the AutoDock docking software. The docking was carried out using the standard settings of AutoDock Vina 1.1.0 (7), and the nine low energy binding modes were retained. The most likely binding pose was selected as the lowest energy pose, which aligned well with the predicted positions of the hot spots.

Ribosome binding assays. Rabbit reticulocyte lysate was preincubated with 0.6 mM cycloheximide (CHX) ±50 μM 4E1RCat for 5 min at 30 °C. [^{32}P]-radiolabeled mRNA was then added

to the reaction and the incubation continued for an additional 10 min at 30 °C. The mRNA templates used in the binding reactions were m^7GpppG-terminated firefly luciferase A^+ and GpppG-terminated Hepatitis C Virus internal ribosome entry site, respectively. Translation complexes were resolved by centrifugation through 10%–30% glycerol gradients in an SW40 rotor at 187,000 × *g* for 3 h. Fractions from each gradient were collected using a Brandel Tube Piercer connected to an ISCO fraction collector. Fractions of 500 μL were collected, and radioactivity determined by scintillation counting.

GST-pull downs. For pull-down experiments, 2.5 μg GST-fusion proteins were incubated in the presence of 100 μM 4E1RCat and 0.25 μg eIF4E. Following incubation for 1 h at RT in Binding Buffer [20 mM $Tris_{7.5}$, 100 mM KCl, 10% glycerol, and 0.1% nonidet P-40 (NP-40)], the reaction was incubated with glutathione beads for another hour. Beads were washed three times with 10-column volumes of Binding Buffer and eluted for 1 h using 10 mM reduced glutathione. The eluents were separated on a 10% SDS-polyacrylamide gel followed by transfer to a PVDF membrane (Millipore) and Western blot analysis. Anti-GST and anti-eIF4E antibodies were from Santa Cruz. Secondary antibodies were from Jackson Immuno Research.

For GST-pulldown experiments using radiolabeled eIF4GI, full-length eIF4GI was generated by in vitro transcription from a full-length cDNA clone containing a T7 RNA polymerase promoter. The resulting mRNA was translated in rabbit reticulocyte lysate (Promega) in the presence of [^{35}S]-methionine. For pull-down experiments, 2.5 μg GST-eIF4E or GST prebound to glutathione beads were incubated with radiolabeled eIF4GI in the absence or presence of 100 μM 4E1RCat in Binding Buffer (50 mM $Tris_{7.5}$, 150 mM NaCl, 10 mM EDTA) for 2 h at 4 °C. Following three washes with 10-column volumes Binding Buffer, bound proteins were eluted for 1 h using 10 mM reduced glutathione. The eluents were analyzed on a 10% SDS-polyacrylamide gel, stained with Coomassie to monitor equal loading, then treated with En^{3}Hance (PerkinElmer), dried, and exposed to X-Omat film (Kodak).

In vivo metabolic labeling. For [^{35}S]-methionine labeling in vivo, 60,000 cells/well were seeded in 24-well plates 24 h prior to treatment. Cells were treated for 4 h in the presence of increasing concentrations of compound. For reversibility assays, cells were incubated for 4 h with 50 μM 4E1RCat, washed with prewarmed PBS, followed by addition of DMEM without 4E1RCat. Cells were allowed to recover for the indicated time points. For the last hour, medium was replaced by methionine-free DMEM supplemented with 10% dialyzed serum and for the last 15 min, cells were labeled with [^{35}S]-methionine (150–225 μCi/ml). Medium was removed, cells washed with PBS and lysed in RIPA buffer (20 mM $Tris_{7.5}$, 100 mM NaCl, 1 mM EDTA, 1 mM EGTA, 0.1% NP-40, 0.5% sodium desoxycholate, 0.1% SDS, 20 mM ß-glycerophosphate, 10 mM NaF, 1 mM PMSF, 4 μg/mL aprotinin, 2 μg/mL leupeptin, and 2 μg/ml pepstatin).

For RNA and DNA labeling, cells were treated for 4 h with 50 μM 4E1RCat in the presence of [^{3}H]-uridine (24 μCi/mL) or [^{3}H]-thymidine (48 μCi/mL). Cells were washed in PBS and lysed in RIPA buffer as described above. Samples were trichloroacetic acid (TCA) precipitated and radioactivity determined by scintillation counting. Protein content in each sample was measured using the BioRad D_C Protein Assay (BioRad Laboratories) and used to standardize the counts obtained after TCA precipitation.

Polysome profile analysis. Twelve million Jurkat cells were seeded in 15 cm^2 dishes in the presence of 50 μM 4E1RCat or vehicle (DMSO) for 1 h. Cells were harvested and processed as described previously (8). For polysome profiling of liver extracts, extracts were prepared as described previously (9).

TUNEL assays. For TUNEL assays, 6–8 w old female C57Bl/6 mice bearing well palpable Pten$^{+/-}$Eμ-Myc lymphomas, were treated three times 12 h apart with 4E1RCat (15 mg/kg) or twice with rapamycin (4 mg/kg). Doxorubicin (10 mg/kg) was included with the last treatment. Six hours after the last injection, tumors were removed and fixed in 10% Neutral Buffered Formalin overnight and embedded in paraffin. Tumor sections (4 μm) were used in TUNEL assays performed according to the manufacturer's instructions (Roche Applied Science), followed by staining of the sections with Hematoxylin.

Cell proliferation and median effect analysis. TSC2$^{+/-}$Eμ-Myc and Eμ-Myc lymphomas were seeded in 96-well plates at 10^6 cells/mL in the presence of increasing concentrations of Dxr (ranging from 3.9 nM to 250 nM) and 4E1RCat (ranging from 78.13 nM to 10 000 nM) at a constant ratio of either 20 : 1 or 40 : 1. Twenty four hours later, a (3-(4,5-dimethylthiazol-2-yl)-5-(3-carboxymethoxyphenyl)-2-(4-sulfophenyl)-2H-tetrazolium) assay was performed. To this end, CellTiter 96 A_{queous} One Solution Cell Proliferation Assay (Promega) was added to the plates and the plates further incubated for up to 3 h, followed by measuring the OD_{490} on a SpectramaxPlus^{384} (Molecular Devices) using Softmax Pro 4.8.2 software. Values obtained were standardized against DMSO controls. Median Effect Analysis was determined using the method of Chou and Talalay (10) using CompuSyn 1.0 (ComboSyn Inc, NJ).

1. Cencic R, Yan Y, Pelletier J (2007) Homogenous time resolved fluorescence assay to identify modulators of cap-dependent translation initiation. *Comb Chem High-Throughput Screen* 10:181–188.
2. Khan RH, Rastogi RC (1991) A convenient and facile synthesis of 2-Arylidene-4-Phenyl-but-3-En-4-Olides by use of N,N-Dimethyl(Chlorosulphonyl)Methaniminium chloride as a cyclodehydrating agent. *Journal of Chemical Research-S* 22:260–260.
3. Egorova AY, Nesterova VV (2005) Synthesis of arylidene derivatives of 1-aryl-3H-pyrrol-2-ones. *Khimiya Geterotsiklicheskikh Soedinenii* 36:1163–1168.
4. Brenke R, et al. (2009) Fragment-based identification of druggable "hot spots" of proteins using Fourier domain correlation techniques. *Bioinformatics* 25:621–627.
5. Dennis S, Kortvelyesi T, Vajda S (2002) Computational mapping identifies the binding sites of organic solvents on proteins. *Proc Natl Acad Sci USA* 99:4290–4295.
6. Landon MR, Lancia DR, Jr., Yu J, Thiel SC, Vajda S (2007) Identification of hot spots within druggable binding regions by computational solvent mapping of proteins. *J Med Chem* 50:1231–1240.
7. Trott O, Olson AJ (2010) AutoDock Vina: improving the speed and accuracy of docking with a new scoring function, efficient optimization, and multithreading. *J Comput Chem* 31:455–461.
8. Cencic R, et al. (2009) Synergistic effect of inhibiting translation initiation in combination with cytotoxic agents in acute myelogenous leukemia cells. *Leuk Res* 34:535–541.
9. Cencic R, et al. (2009) Antitumor activity and mechanism of action of the cyclopenta[b] benzofuran, silvestrol. *PLoS ONE* 4:e5223.
10. Chou T, Talalay P (1984) Quantitative analysis of dose-effect relationships: the combined effects of multiple durgs or enzyme inhibitors. *Adv Enzyme Regul* 22:27–55.

A

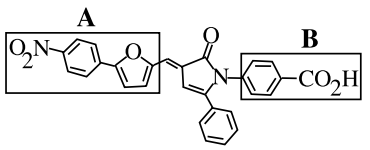

4E1RCat

B

Compound ID	A	B	TR-FRET IC_{50} [μM]
resynthesized 4E1RCat	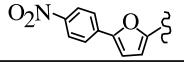	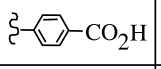	3.2
JM2-147B	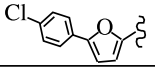	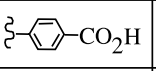	12.8
JM2-147C	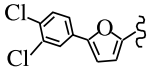	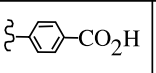	7.2
JM2-147D	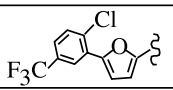	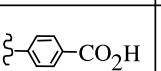	6.4
JM2-151	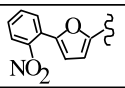	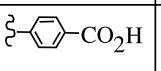	12.7
JM2-154A	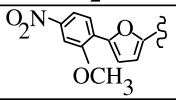	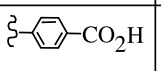	19.3
JM2-154B	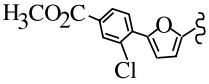	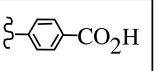	7.4
STOCK2S-26027	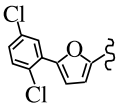	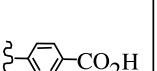	3.3

Compound ID	A	B	TR-FRET IC_{50} [μM]
JM2-103A	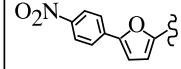	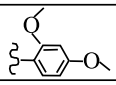	>50
JM2-103C	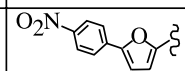	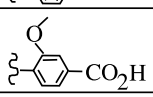	9.4
JM2-149	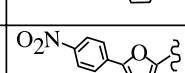	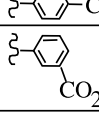	6.1
STOCK2S-32086	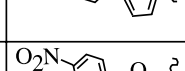		>50
STOCK2S-35315	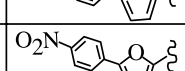	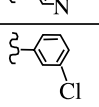	>50
STOCK2S-45520	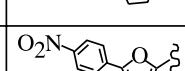		>50
STOCK2S-49506	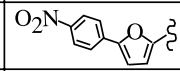		>50
STOCK2S-45619	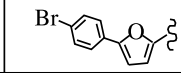	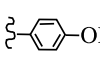	>50
JM2-90	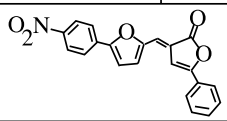		~50

Fig. S1. *SAR analysis of 4E1RCat. A.* Schematic diagram of 4E1RCat denoting moieties "A" and "B" that were targeted for SAR analysis. *B.* Structures of 4E1RCat analogs and corresponding IC_{50}'s from the TR-FRET assay.

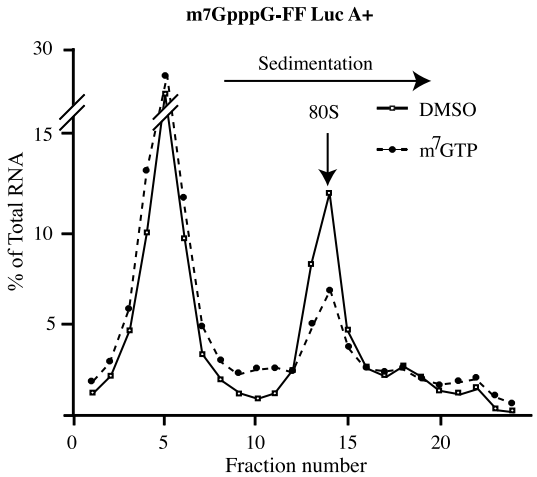

Fig. S2. *Inhibition of cap-dependent ribosome binding by* m^7GTP. ^{32}P-labeled m^7GpppG-FF Luc A^+ RNA was incubated with CHX and vehicle (1% DMSO) or 1.5 mM m^7GTP in rabbit reticulocyte lysate. Following separation on sucrose gradients, fractions were collected and radioactivity determined. Total counts recovered from each gradient and the percent mRNA bound in 80S complexes were: m^7GpppG-FF/mRNA + 1% DMSO [63,096 cpm, 28% binding] and m^7GpppG-FF/mRNA + m^7GTP [55,045 cpm, 16.4% binding].

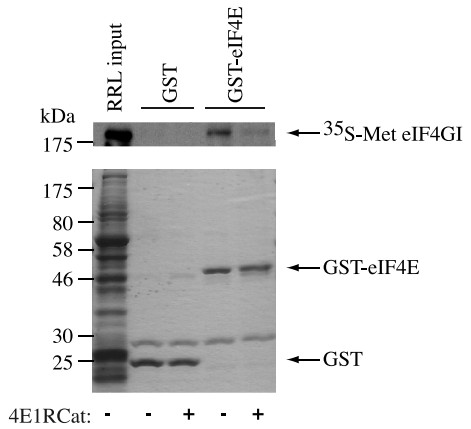

Fig. S3. *Inhibition of GST-eIF4E and eIF4GI interaction by 4E1RCat.* GST-pull downs were performed with radiolabeled eIF4GI produced from in vitro translation reactions in rabbit reticulocyte lysate (RRL). Lane 1, 1/5 of input material used for pull-down experiments; Lanes 2-5 are eluents from GST-pull-down experiments utilizing GST (lanes 2, 3) or GST-eIF4E (lanes 4, 5) as bait. The presence or absence of 4E1RCat is indicated. Top: Autoradiography of gel showing radiolabeled eIF4GI. Bottom: Coomassie brilliant blue staining of input RRL (lane 1) and GST-tagged proteins (lanes 2-5).

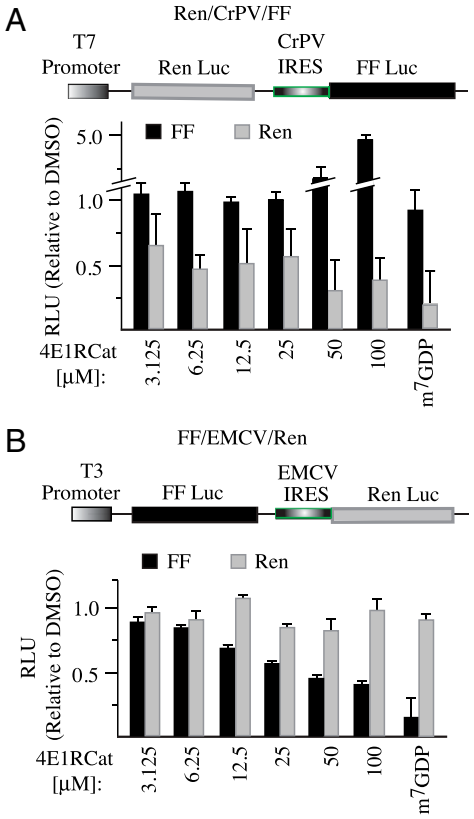

Fig. S4. *In vitro translations performed in Krebs extracts programmed with Ren/CrPV/FF or FF/EMCV/Ren.* A schematic representation of Ren/CrPV/FF (*A*) and FF/EMCV/Ren (*B*) mRNAs is provided (top). In vitro translations were performed as described for Fig. 4*A*. Bottom: FF and Ren, renilla (Ren) luciferase (luc) activity (RLU), values (relative to DMSO controls) from two independent experiments with the SEM are provided.

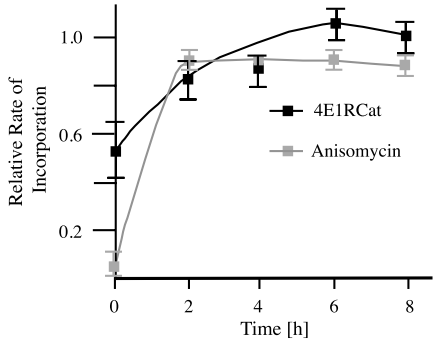

Fig. S5. *Inhibition of translation by 4E1RCat is reversible*. The rate of ^{35}S-Met incorporation into TCA-insoluble material in HeLa cells was measured and is expressed relative to vehicle (DMSO) treated cells. Results are the average of three experiments with the SEM shown.

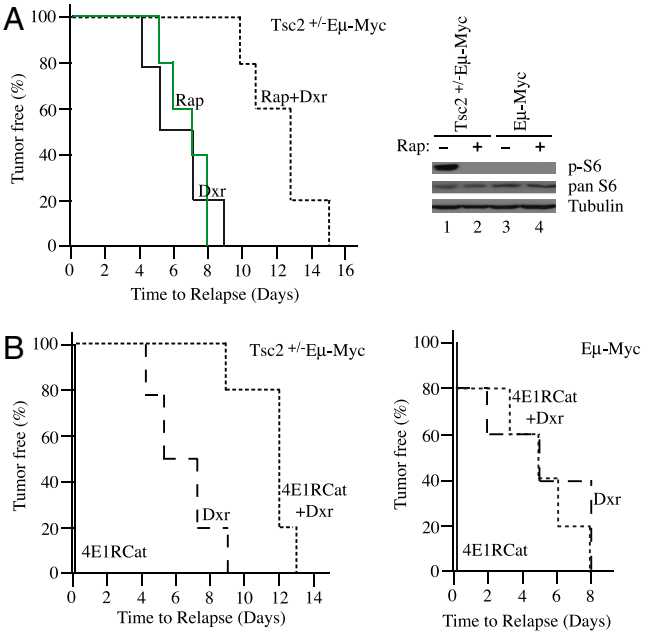

C

Cell line	Combination	Ratio	CI(ED50)	CI(ED75)	CI(ED90)
Eμ-Myc	4E1RCat+Dxr	20:1	>10	>10	>10
	4E1RCat+Dxr	40:1	>10	>10	>10
Tsc2 +/-Eμ-Myc	4E1RCat+Dxr	20:1	0.59	0.52	0.46
	4E1RCat+Dxr	40:1	0.66	0.59	0.53

Fig. S6. *4E1RCat synergizes with Dxr in vitro and in vivo in* Tsc2$^{+/-}$Eμ-Myc *lymphomas*. (*A*) Kaplan-Meier plot (left) showing tumor free survival of mice bearing Tsc2$^{+/-}$Eμ-Myc tumors following treatment with Dxr (solid black line; $n = 4$), Rap (solid green line; $n = 5$), or Rap + Dxr (dashed black line; $n = 5$; $p = 0.003$). Right: Tsc2$^{+/-}$Eμ-Myc or Eμ-Myc cells were treated for 2 h with 20 nM rapamycin followed by Western blot analysis probing for phospho-S6 (p-S6). (*B*) Kaplan-Meier plot showing tumor free survival of mice bearing Tsc2$^{+/-}$Eμ-Myc or Eμ-Myc tumors following treatment with 4E1RCat, Dxr or 4E1RCat + Dxr (For Tsc2$^{+/-}$Eμ-Myc lymphomas; $p < 0.001$). $n = 5$ in all cohorts (*C*) Lymphoma cells of the indicated genotypes were treated with a constant ratio of Dxr and 4E1RCat for 24 h, at which point cell viability was determined using a (3-(4,5-dimethylthiazol-2-yl)-5-(3-carboxymethoxyphenyl)-2-(4-sulfophenyl)-2H-tetrazolium) assay and Median Effect Analysis calculated as described in *SI Materials and Methods*. Combination Index (CI) values below 1 indicate synergism, whereas CI values above 1 indicate antagonism. Average of duplicates are presented.

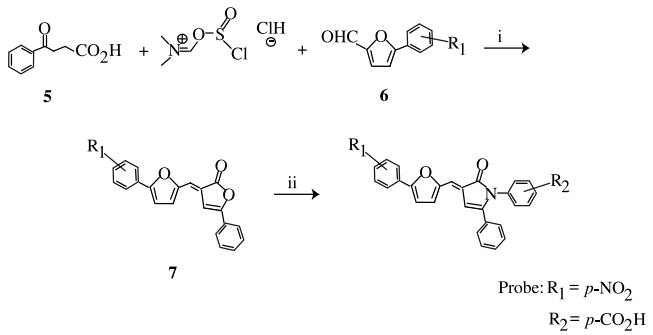

Fig. S7. *Representative synthetic scheme for 4E1RCat and its analogs*. Reagents and conditions: (*i*) TEA/DCM, 5 h, 25 °C; (*ii*) substituted anilines, MW, 150W, 2 h, 180 °C.